Electronic Supplementary Material (ESI) for RSC Advances.
This journal is © The Royal Society of Chemistry 2022

Supplementary Information

Exploiting Directed Self-Assembly and Disassembly for off-to-on Fluorescence Responsive Live Cell Imaging

Niamh Curtin,[1] Massimiliano Garre,[1] Jean-Baptiste Bodin,[2] Nicolas Solem,[3] Rachel Méallet-Renault,[2] Donal F. O'Shea[1*]

[1] Department of Chemistry, RCSI, 123 St Stephen's Green, Dublin 2, Ireland.

[2] Université Paris-Saclay, Institut des Sciences Moléculaires d'Orsay (ISMO), CNRS, 91400 Orsay, France.

[3] Université Paris-Saclay, CNRS, Institut des Sciences Moléculaires d'Orsay, 91405, Orsay, France.

Contents

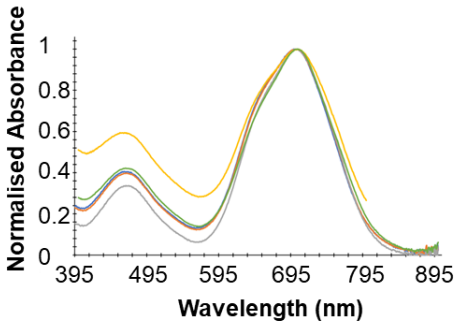

Figure S1. Stability of aqueous NP**1**-P_{188} solutions. Absorption spectra of NP**1**-P_{188} (5 μM) taken 4 (blue), 7 (orange), 17 (grey), 27 and 44 (green) days post synthesis.

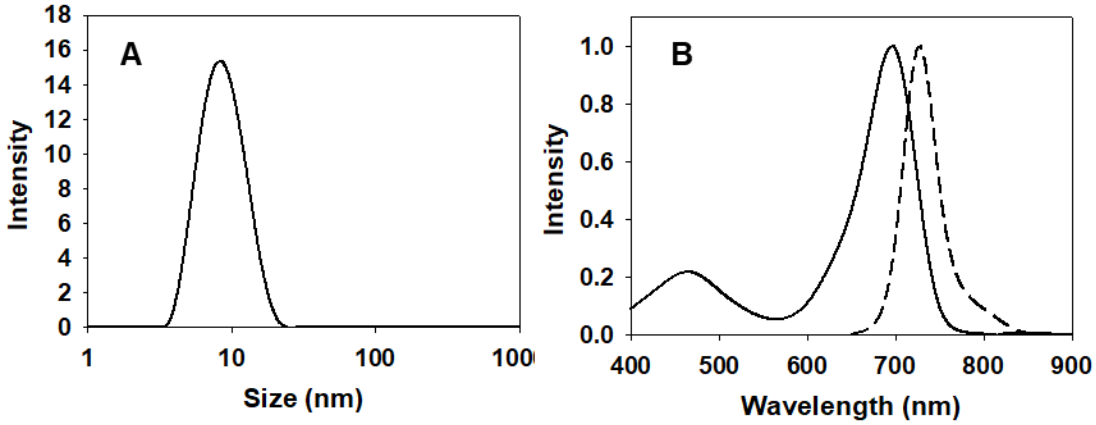

Figure S2. Physical and photophysical characteristics of M**1**-PS_{20}. (**A**) DLS trace of M**1**-PS_{20} (5 μM) at 25 °C (**B**) Absorbance (black) and emission (black dashed) of M**1**-PS_{20} (5 μM)

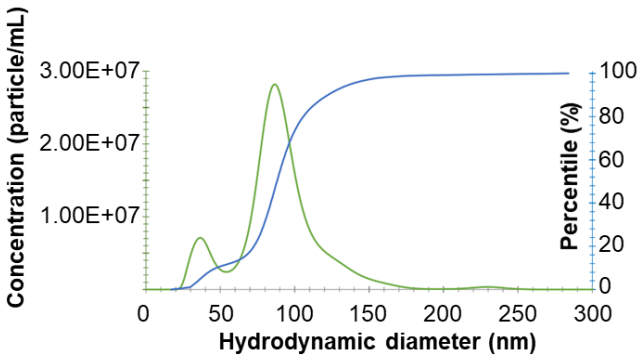

Figure S3. Nanoparticle tracking analysis of NP**1**-P_{188} (green, conc of **1** and P_{188}) solution, and the percentile of the population (blue). A total 136,098 particles analysed.

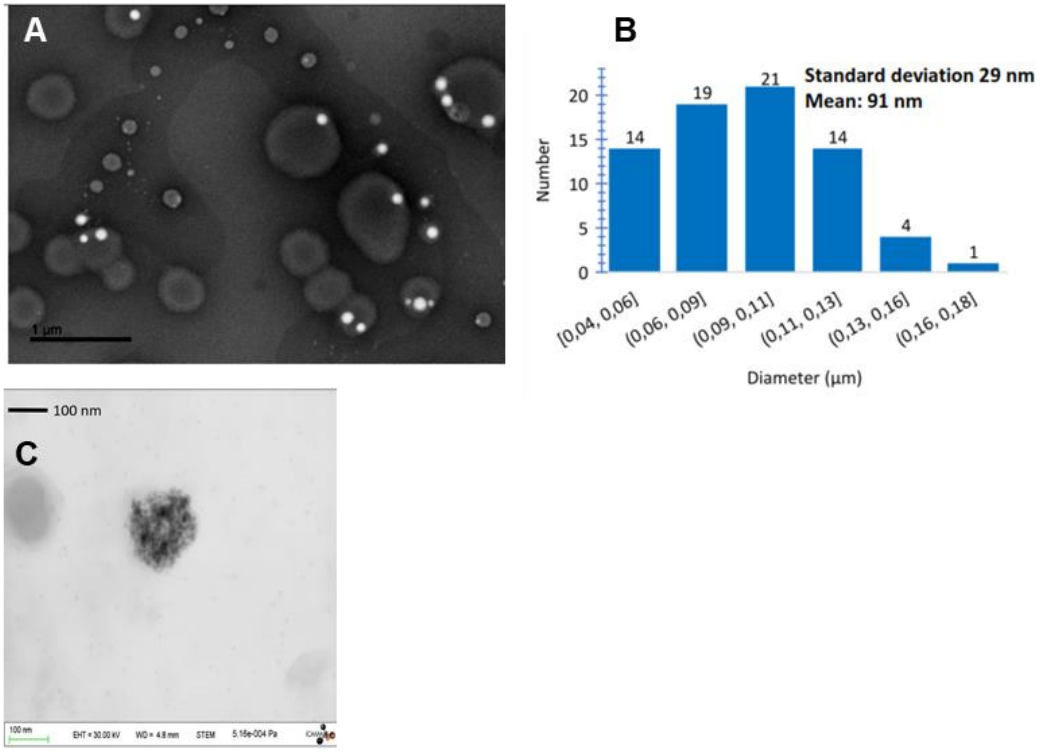

Figure S4. Scanning transmission electronic microscope (STEM) images of NP**1**-P_{188} (P = $5{,}07.10^{-4}$ Pa, tension = 30,0 kV). (**A**) After treatment with phosphotungstic acid (PTA) for negative staining. (**B**) Histogram of the different sizes measured in six different TEM images including the image shown, the total number of particles analysed was 73. (**C**) TEM image without staining showing an individual nanoparticle showing potential aggregates of **1** as darkened areas. Scale bar 100 nm.

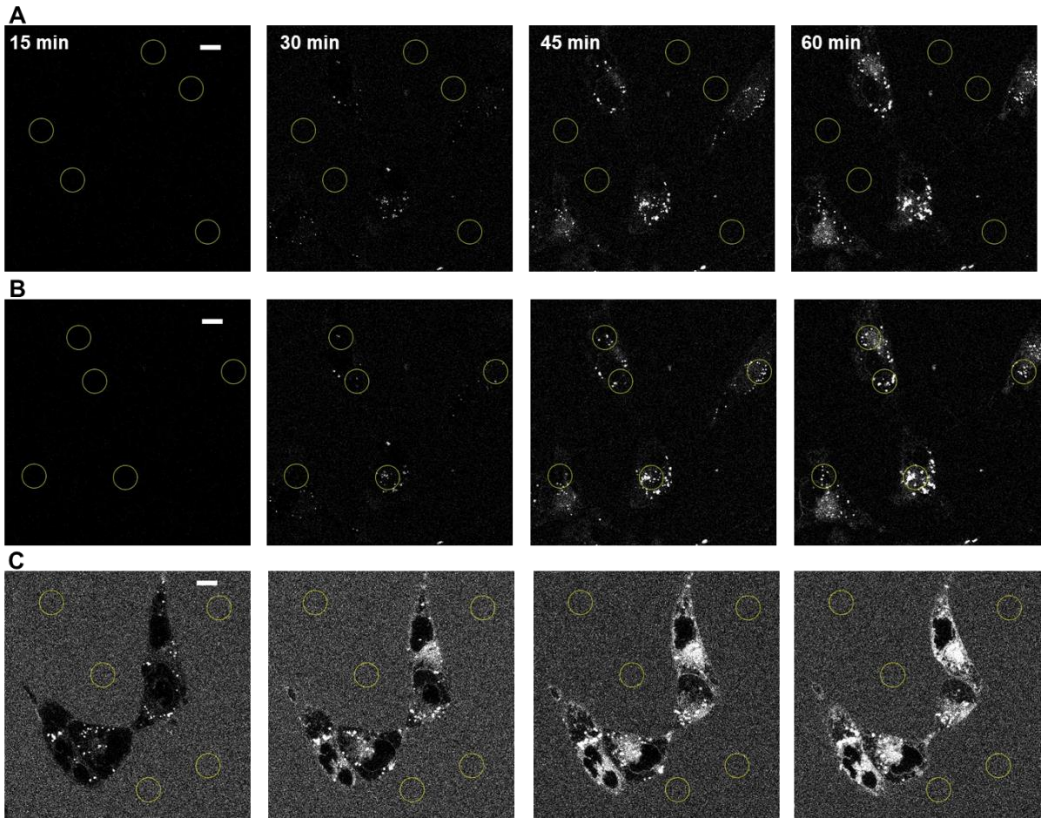

Figure S5. Time course of confocal imaging illustrating low background of NP**1**-P_{188} in comparison to M**1**-PS_{20}, yellow circles indicate extra and intra cellular areas used for intensity measurements, scale bar 10 µm. (**A**) NP**1**-P_{188} extra-cellular circles (**B**) NP**1**-P_{188} intra-cellular circles (**C**) M**1**-PS_{20} extra-cellular circles

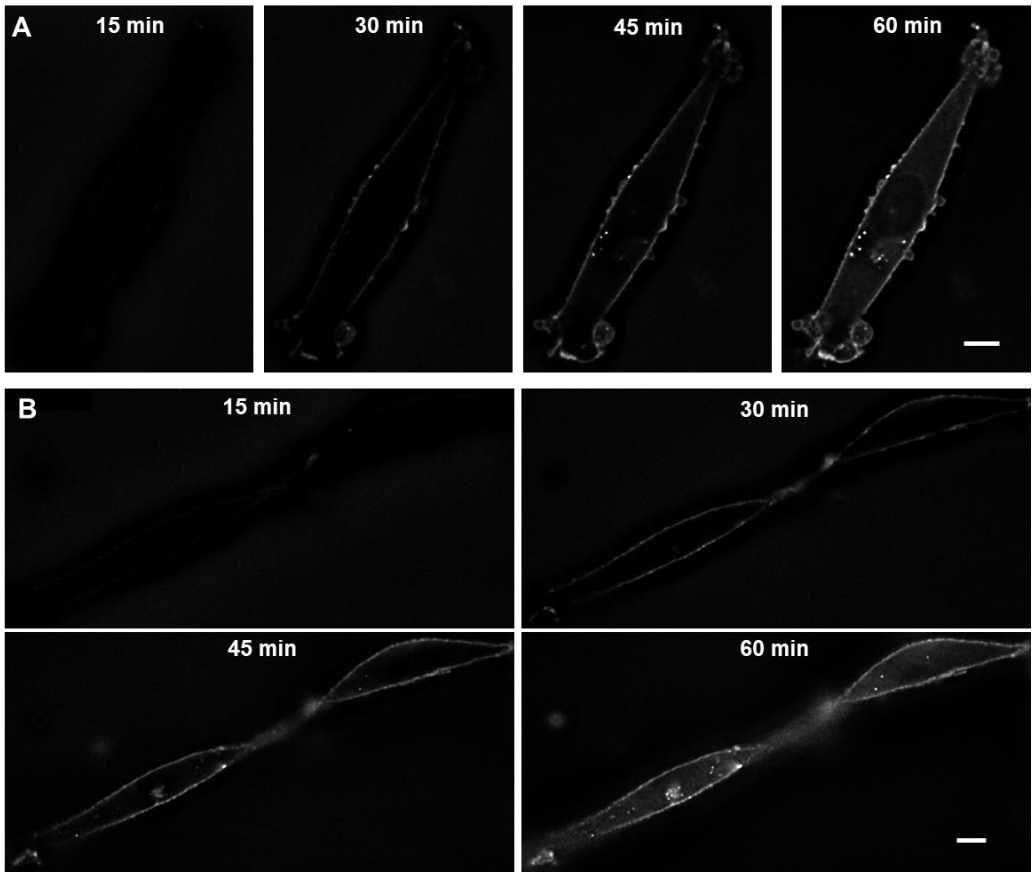

Figure S6. Widefield imaging (processed Huygens) of fixed MDA-MB 231 at 37 °C cells treated with NP**1**-P_{188} at 15, 30, 45, 60 min time points showing staining of the plasma membrane in (**A**) and (**B**) duplicate experiment. See SI Movie S2 and S2A for video.

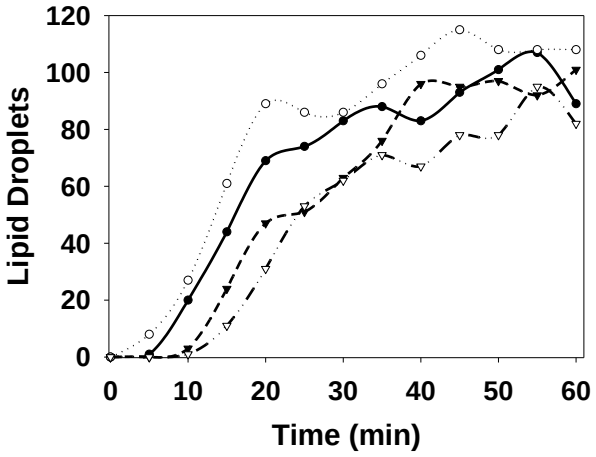

Figure S7. Graphed plot of four MDA-MB 231 cells showing the increase in number of LDs visible over 60 min following live cell treatment with NP**1**-P_{188}.

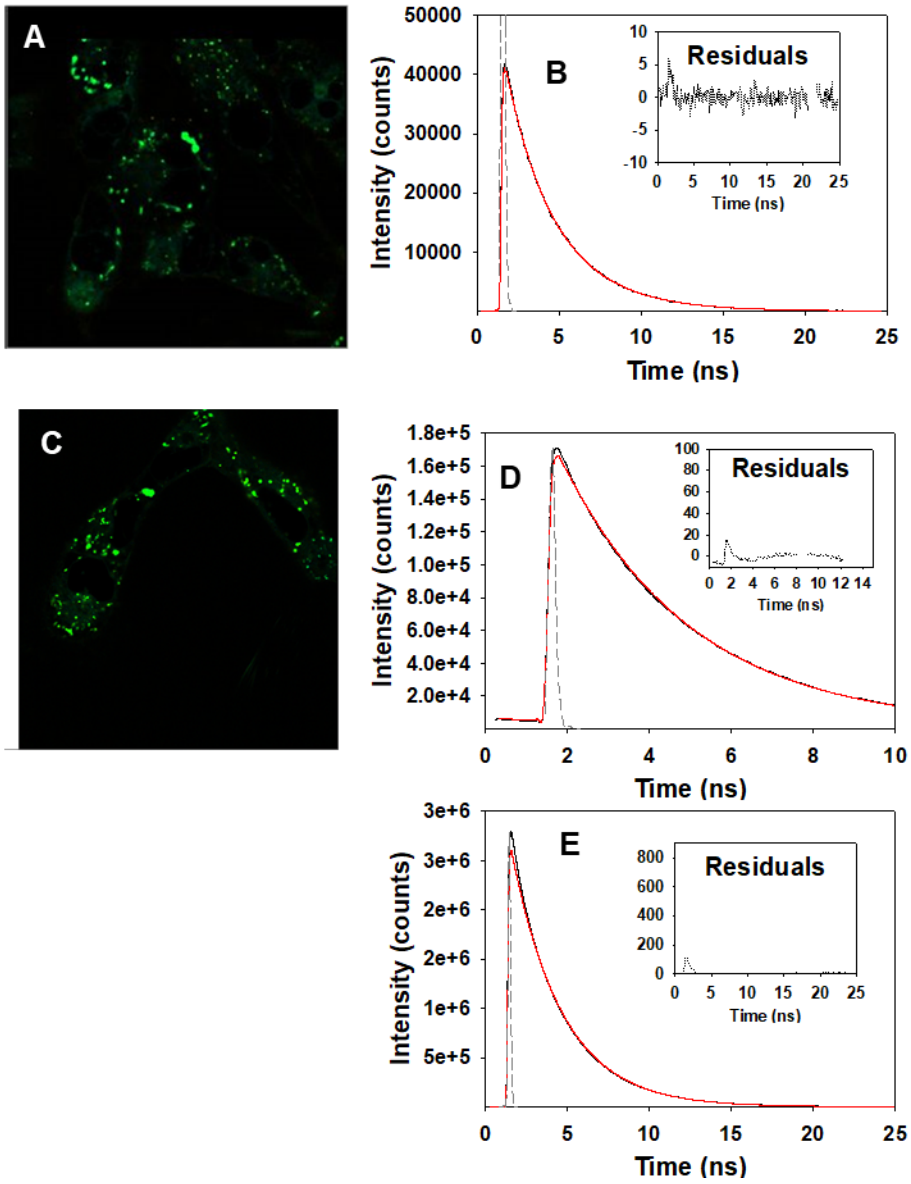

Figure S8. (**A**) FLIM imaging of LDs in live MDA-MB 231 cells 60 min following treatment with NP**1**-P_{188}. (**B**) Mono-exponential fitted fluorescence lifetime decays from LDs (red trace fitted data, grey IRF), (**C**) Repeat experiment of FLIM imaging of LDs in live MDA-MB 231 cells 60 min following treatment with NP**1**-P_{188} (**D**) Repeat experiment of mono-exponential fitted fluorescence lifetime decays from FOV (red trace fitted data grey IRF) (**E**) Mono-exponential fitted fluorescence decay of **1** in triolein solution (red trace fitted data, grey trace IRF)

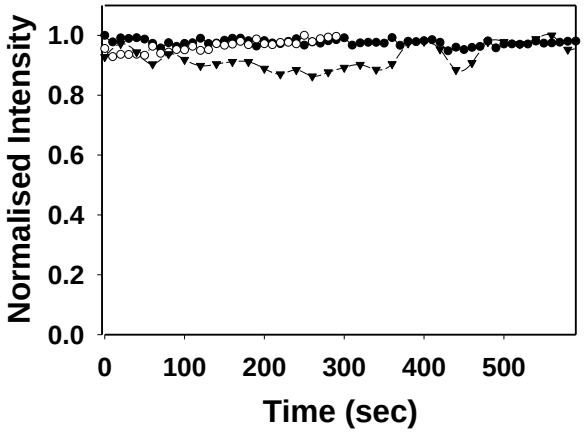

Figure S9. Stability demonstration of **1**. Normalised continual integrated fluorescence intensity from a three different cell FOVs during continuous imaging.

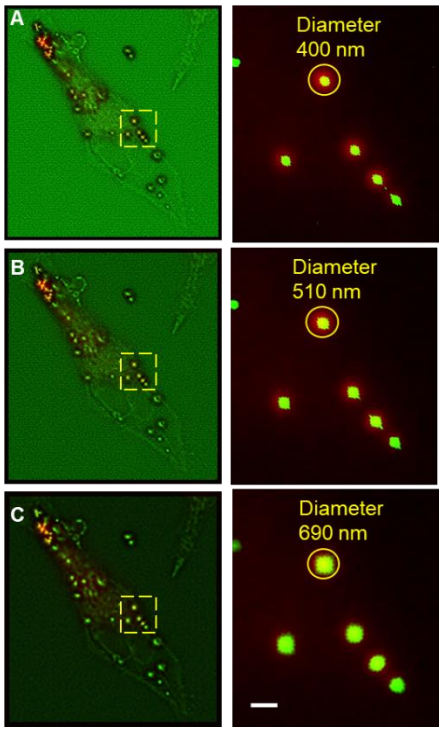

Figure S10. Optimization of Super resolution radial fluctuations (SRRF) imaging parameters using ring radius (**A**) 0.5, (**B**) 1 and (**C**) 2. Overlap of SRRF image (green) with original NIR image (red). Effect of ring radius parameter seen through changes in LD diameter, scale bar 1 μm

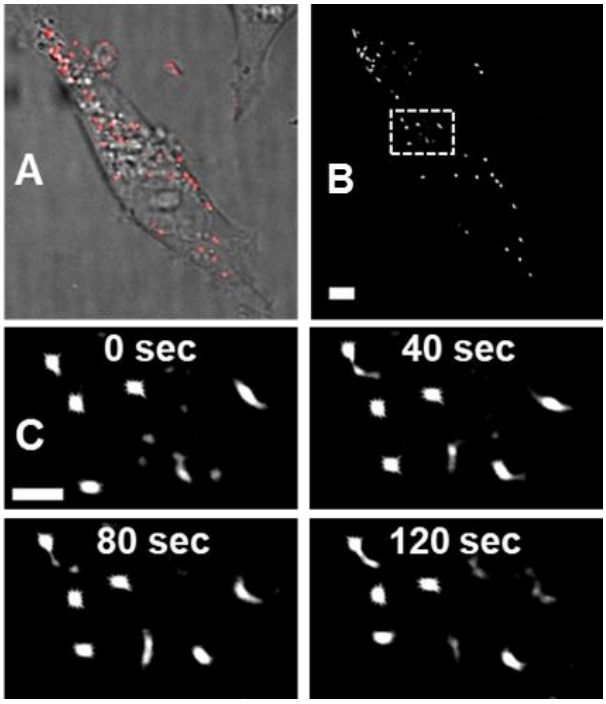

Figure S11. SRRF imaging of LDs in MDA-MB 231 cells, incubated with NP**1**-P_{188} for 2 h. (**A**) DIC image with fluorescent LDs overlay shown in red. (**B**) Fluorescence image of LDs (white) stained by **1** following 2 h incubation with NP**1**-P_{188}, scale bar 5 µm. (**C**) Time course of SRRF imaging of live cells showing motion of LDs (white), scale bar 2 µm. See SI Movie S4.

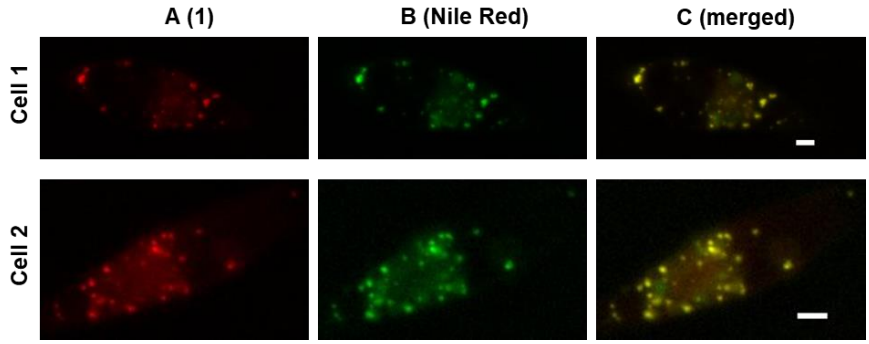

Figure S12. Widefield fluorescence images of cells co-incubated with (**A**) NP**1**-P_{188} and (**B**) nile red for 1 h and fixed with 4% formaldehyde. (**C**) Merged images of and **1** (red) and nile red (green) showing co-localisation (yellow) of fluorophores in LDs. Scale bar 5 µm

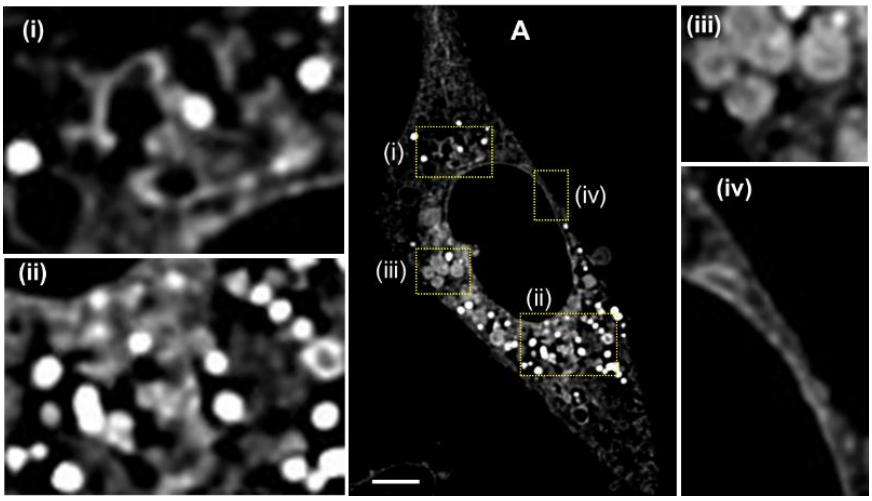

Figure S13. CLSM image showing an MDA-MB 231 fixed cell following 24 h incubation with NP**1**-P_{188}. (**A**) Whole cell with fluorescence shown in white for clarity, scale bar 5 µm**,** (**i, ii**) ER network with LDs, (**iii**) large vacuoles (**iv**) nuclear membrane

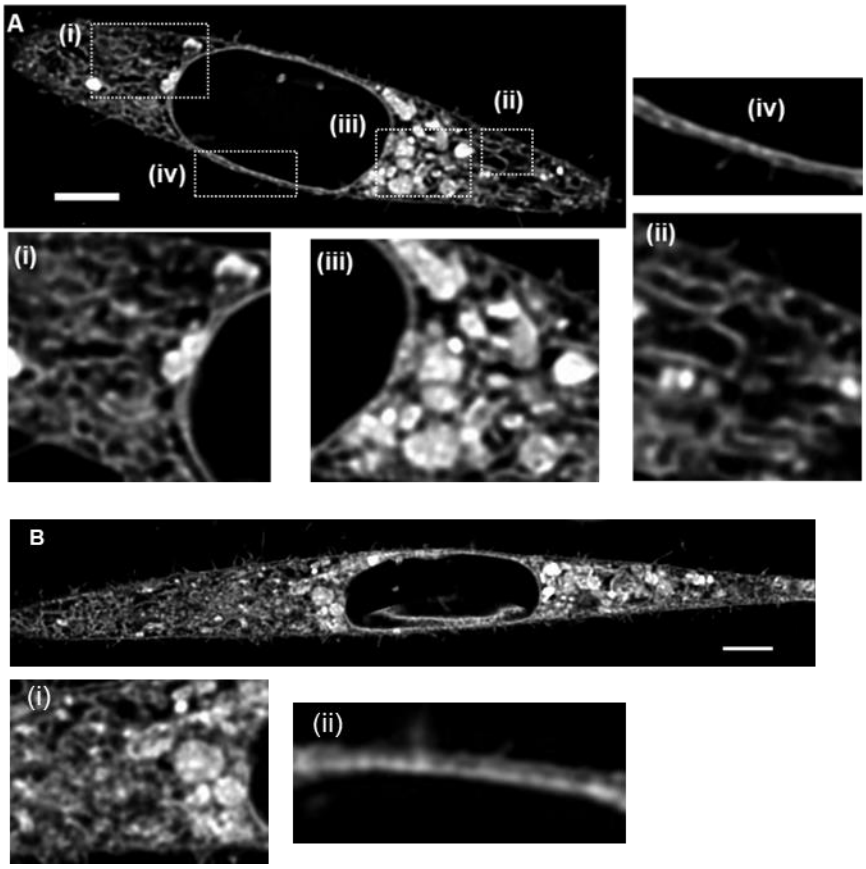

Figure S14. CLSM image of starved MDA-MB 231fixed cells treated with NP**1**-P_{188} for 24 h. (**A**) whole single cell view with labelled expansion areas. (**i**) and (**ii**) cell regions with few LDs and ER visible, (**iii**) secretory granules, (**iv**) nuclear membrane, scale bar 5 µm (**B**) whole single

cell view with labelled expansion areas (**i**) ER and secretory granules (**ii**) nuclear membrane, scale bar 5 µm

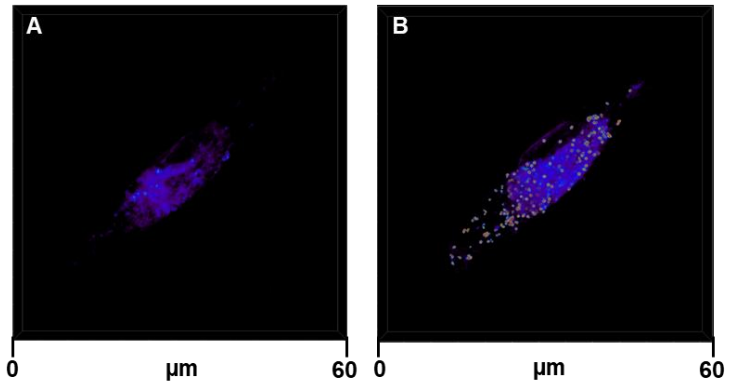

Figure S15. CLSM 3D image of starved live MDA-MB 231 cell treated with NP**1**-P_{188} for 3h (**A**) before addition of oleic acid (**B**) after addition of oleic acid for 30 min

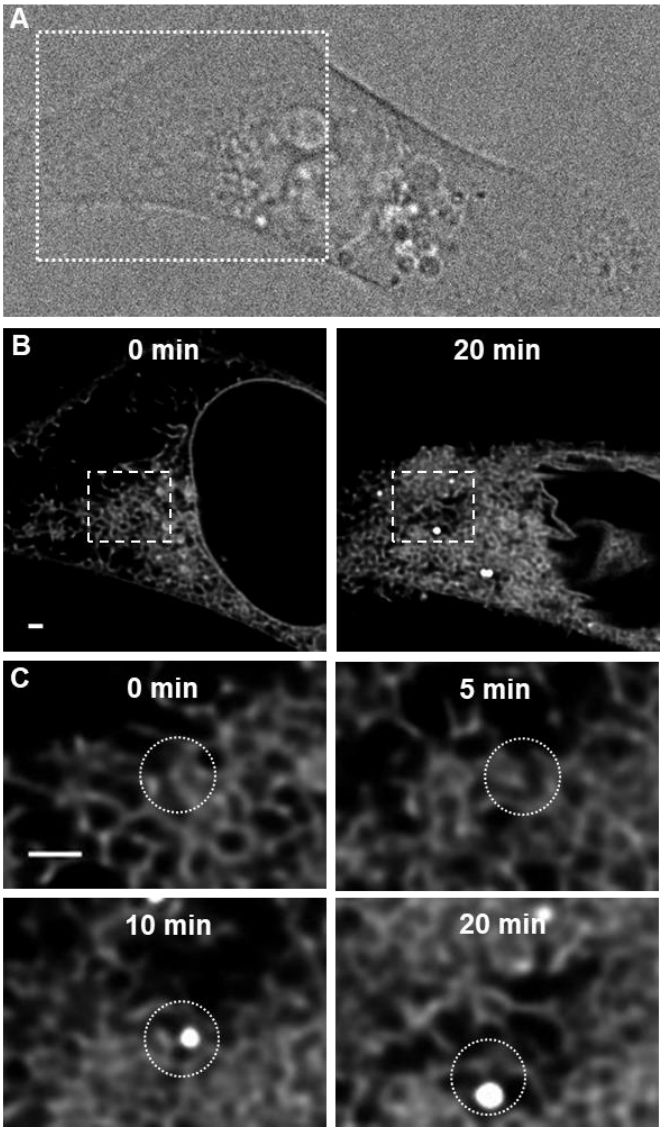

Figure S16. (**A**) DIC image of starved live MDA-MB 231 cell treated with NP**1**-P_{188} for 3h, (**B**) CLSM image showing growth of LD seen following addition of oleic acid to media over 20 min (**C**) Expansion of box showing LD biogenesis from ER at 0, 5, 10, 20 min, scale bar 1 µm. See SI Movie S8 for video.

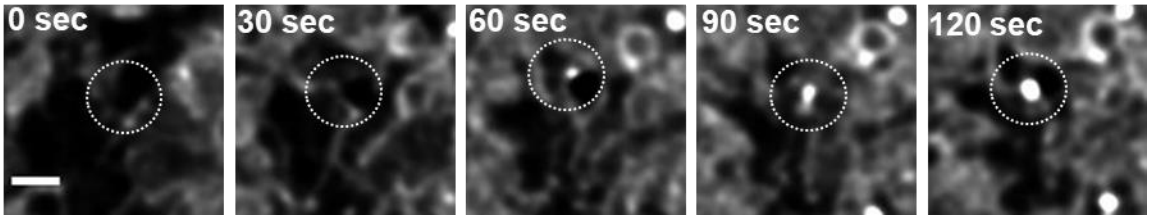

Figure S17. CLSM image showing growth of LD from ER following addition of oleic acid to media at 0, 30, 60, 90, and 120 sec, scale bar 1 µm. See SI Movie S8A for video.

A

Solvent	Polarity Index	Ratio (I / III)
Cyclohexane	0.2	0.70
Toluene	2.4	1.30
Dichloromethane	3.1	1.47
Tetrahydrofuran	4	1.45
Ethanol	5.2	1.34
Acetonitrile	5.8	1.94
Water*	10.2	1.92

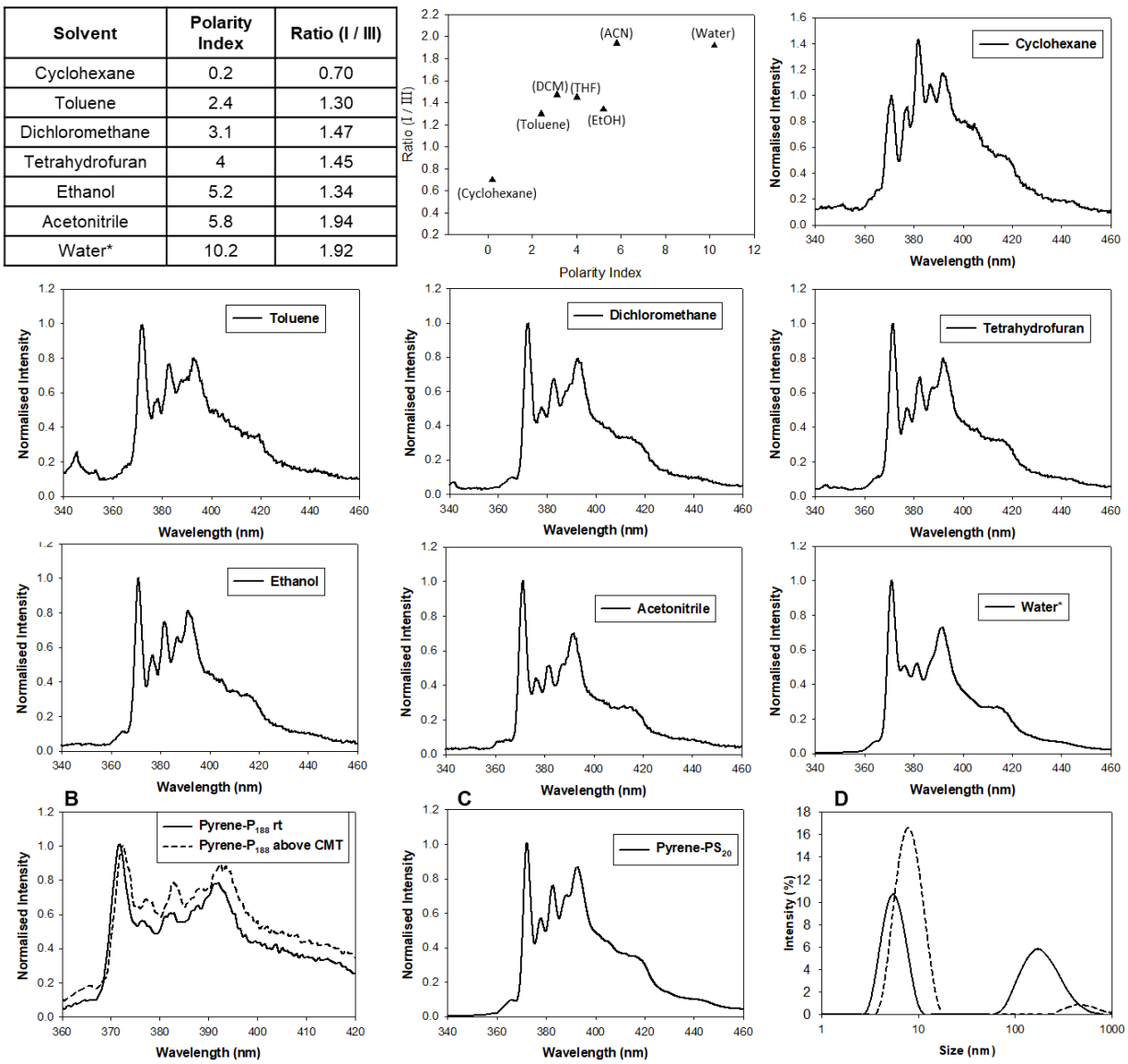

Figure S18. Investigation of NP micro-environment using pyrene (**A)** Emission spectra of pyrene (0.5 µM) in different solvents used to create polarity table index to ratio of 1st to 3rd band (**B**) Emission NP-pyrene-P_{188} (5 µM, 1.18 mM) at rt and 65 °C (**C**) Emission pyrene-PS_{20} (5 µM , 8.14 mM) at rt (D) DLS of NP-pyrene-P_{188} (solid) and pyrene-PS_{20} (dashed) at 25 °C

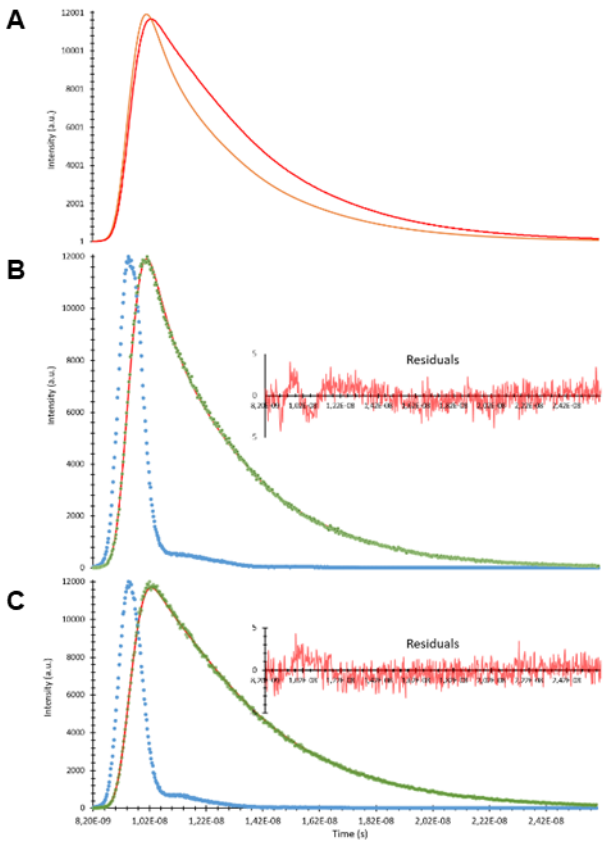

Figure S19. (**A**) Superposition of fitted curve of fluorescent decay of aqueous NP**1**-P_{188} (5 µM, 1.18 mM) using a bi-exponential fitting (orange) and of **1** (5 µM) in $CHCl_3$ using a mono-exponential fitting (red), excitation at 667 nm, emission observed at 710 nm. (**B**) Fluorescent decay (green) of NP**1**-P_{188} and the fitted curve (red). (**C**) Fluorescent decay (green) of **1** in $CHCl_3$ and the fitted curve (red).

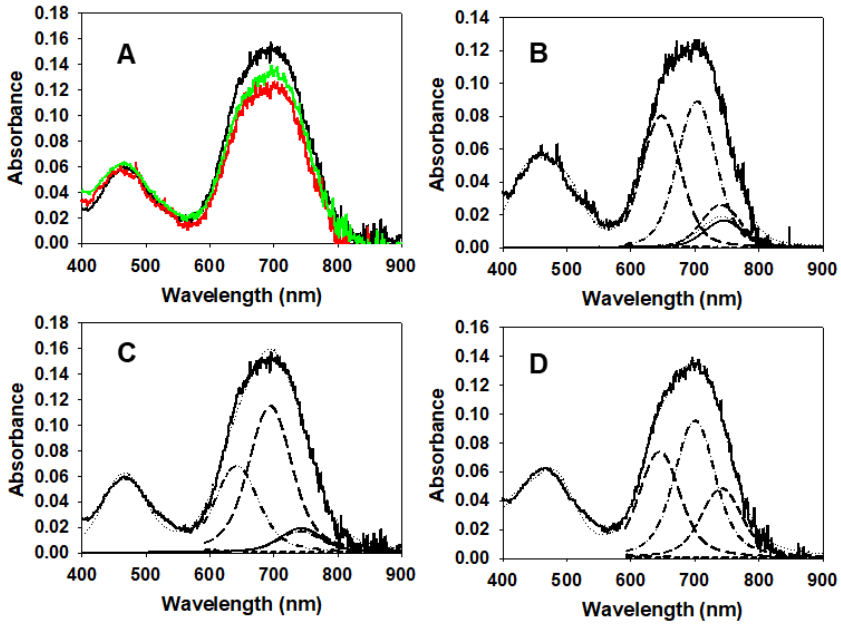

Figure S20. (A) Absorption bands of **1** after 60 min in THF/water 2:98 (black) 5:95 (red) 10:90 (green) (**B**) Voigt function peak fitting of **1** absorption band in THF/water 2:98 showing three contributing bands centred at 642, 695 ~ 742 nm (**C**) Voigt function peak fitting of **1** absorption band in THF water 5:95 showing three contributing bands centred at 648, 703 ~ 743 nm and (**D**) Voigt function peak fitting of **1** absorption band in THF/water 10:90 showing three contributing bands centred at 645, 700, 742 nm.